

Neutron Reflectometry on Interfacial Structures of the Thin Films of Polymer and Lipid

Naoya TORIKAI,^{1,†} Norifumi L. YAMADA,¹ Atsushi NORO,² Masashi HARADA,^{2,††}
Daisuke KAWAGUCHI,² Atsushi TAKANO,² and Yushu MATSUSHITA²

¹*Institute of Materials Structure Science, High Energy Accelerator Research Organization,
1-1 Oho, Tsukuba 305-0801, Japan*

²*Department of Applied Chemistry, Graduate School of Engineering, Nagoya University,
Furo-cho, Chikusa-ku, Nagoya 464-8603, Japan*

(Received August 1, 2007; Accepted September 27, 2007; Published November 2, 2007)

ABSTRACT: Neutron reflectometry is a very powerful and essential technique for the studies on material interfaces due to its high spatial resolution, \sim a few tenths of nm , along the depth direction. The use of neutron as a probe is a big advantage for structural analysis on soft-materials, since the scattering contrast can be highly enhanced in hydrogenous materials such as polymers, surfactants, lipids, proteins, etc., without big changes in their physical and chemical properties by substituting all or part of the hydrogen atoms in the molecules with deuterium (a deuterium labeling method). Furthermore, the neutron reflectometry can explore deeply-buried interfaces such as solid/liquid interfaces in a non-destructive way, and make *in situ* measurements combined with various sample environments due to its high transmission to the materials. In this article, the neutron reflectometry is reviewed from the standpoint of researches on interfacial structures of the thin films of polymer and lipid, and its future prospects at a high-intensity pulsed-neutron source are presented. [doi:10.1295/polymj.PJ2007113]

KEY WORDS Neutron Reflectometry / High Depth Resolution / Soft-material / Deuterium Labeling / Non-destructive Exploration / Deeply-buried Interface / *In situ* Measurement /

At interfaces, materials often exhibit different structures or physical properties from in bulk because they interact directly with different materials or phases in a very narrow space. So far many interesting phenomena relevant to interfaces have been reported, *e.g.*, lower surface glass transition temperature, de-wetting, surface segregation, etc., in the research field of soft-materials.^{1,2} Also, material interfaces contribute largely to many practical phenomena known as coating, painting, adhesion, lubrication, etc. In addition, the recent development of nano-technology makes the size of practical devices smaller, so that interfaces occupy the larger proportion of space in the devices, and then play an important role in the device performance. Therefore, strong demands to clarify the structures and physical properties of materials at interfaces have been rapidly grown.

However, in reality it is generally difficult to observe detailed interfacial structure, since the interfacial region is very narrow and has considerably small volume in materials. The material interfaces are not always exposed to air surface, but are deeply buried in materials. Neutron reflectometry is a very powerful and indispensable technique to the studies on material

interfaces because of its high spatial resolution, \sim a few tenths of nm , along the depth direction. Here, the neutron reflectometry is reviewed from the standpoint of soft-material researches by highlighting experimental examples on the thin films of polymer and lipid systems, and its future prospects at a high-intensity pulsed-neutron source are presented.

NEUTRON REFLECTOMETRY

Neutron has unique properties as a probe for structural analysis of materials, compared with electromagnetic waves such as light or X-ray. The neutron is scattered through atomic interaction with nuclei, not electrons, so that scattering length, b , of element is not simply proportional to the atomic number Z , and also isotopes have different b values for neutron.³ Especially, there is a big difference in b between hydrogen (H, $b = -3.74 \times 10^{-15}$ m) and its isotope, deuterium (D, $b = +6.67 \times 10^{-15}$ m), and this gives a big advantage for soft-material researches on polymers, surfactants, lipids, proteins, etc., that possess many hydrogen atoms. The contrast for neutron can be introduced in these hydrogenous molecules with no big

[†]To whom correspondence should be addressed (Tel: +81-29-864-5614, Fax: +81-29-864-3202, E-mail: naoya.torikai@kek.jp).

^{††}Present Address: Toyota Central R&D Laboratories, Incorporated, Nagakute-cho, Aichi-gun 480-1192, Japan

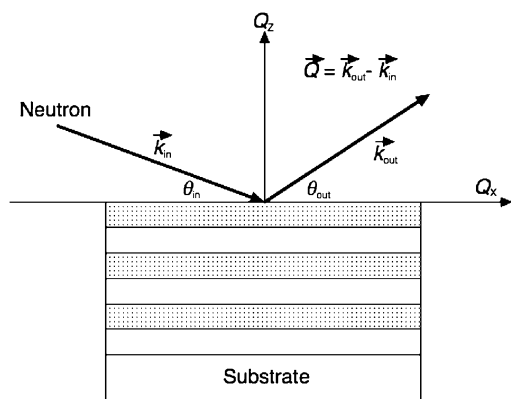


Figure 1. A schematic illustration of the geometrical configuration in a reflectivity measurement.

changes in their physical and chemical properties by substituting the part or all of the hydrogen atoms with deuterium in the molecules (a deuterium labeling method). The contrast matching is also a quite useful concept, in which the contrast of one component is matched with the others by blending the deuterated and normal species at adequate ratio. Another important feature is that neutron has very high transmission to materials, *e.g.*, transmissivity is still kept about 0.5 even though the neutron passes through a silicon block with 50 mm length, so that deeply buried interfaces such as solid/liquid interfaces with a block of silicon or quartz can be explored in a non-destructive way. Also, it is easy to combine neutron experiment with various sample environments such as a vacuum, a vapor, a pressure, etc., requiring the tight seal for a sample cell.

In a reflectivity measurement, a well-collimated neutron beam is incident on optically flat surface of a sample with the small grazing incident angle, θ_{in} , and generally specular reflection, in which the reflection angle, θ_{out} , is equal to θ_{in} , as schematically illustrated in Figure 1, is observed as a function of neutron momentum transfer, $Q_z (= (4\pi/\lambda) \sin \theta_{in})$, where λ is the wavelength of neutron), along the direction perpendicular to the sample surface to probe the depth structure of material with high spatial resolution, \sim a few tenths of *nm*. At the angular position of $\theta_{in} \neq \theta_{out}$, very weak signal of off-specular reflection originating from the in-plane structure along the Q_x -direction shown in Figure 1 can be observed. The refractive index, n , of material for neutron is expressed with its scattering length density, $\rho(\Sigma b_i)$ (nm^{-2}), as

$$n^2 = 1 - 4\pi\rho(\Sigma b_i)/k^2$$

where ρ is the number density, (Σb_i) is a sum of b over the constituent elements of the material, and k is the wave vector defined as $2\pi/\lambda$. Generally, specular reflectivity profile exhibits total reflection with reflectivity of unity, up to the critical Q_z defined as

Table I. The values of $\rho(\Sigma b_i)$ and the critical Q_z for total reflection of typical materials

Materials	$\rho(\Sigma b_i)$ ($\times 10^{-4} \text{ nm}^{-2}$)	Critical Q_z (nm^{-1})
Silicon Si	2.07	0.10
Quartz SiO ₂	4.18	0.14
Nickel Ni	9.21	0.22
Water H ₂ O	-0.56	—
Deuterated water D ₂ O	6.35	0.18
Polyisoprene (C ₅ H ₈) _n	0.27	0.04
Poly(trimethylsilylstyrene-d ₉) (C ₁₁ SiH ₇ D ₉) _n	3.6	0.13
Dimyristoylphosphatidylcholine DMPC	5.17 ^[1]	0.16
Sodium Iodide NaI	1.31	0.081
Poly(styrene-h ₈) (C ₈ H ₈) _n	1.41	0.084
Poly(styrene-d ₈) (C ₈ D ₈) _n	6.47	0.18
Poly(2-vinylpyridine) (C ₇ NH ₇) _n	1.95	0.099

[1] The number density of DMPC was calculated from the molar volume evaluated in aqueous solution experimentally.⁴

$(16\pi\rho(\Sigma b_i))^{1/2}$, when the neutron is incident on the objective interface from the side of the material with lower n . The values of $\rho(\Sigma b_i)$ and critical Q_z for total reflection are tabulated for several materials in Table I. In most cases, specular reflectivity profile is analyzed by a conventional model fitting method with the Parratt's recursion algorithm⁵ or optical matrix formula,⁶ providing the $\rho(\Sigma b_i)$ distribution along the Z depth direction. The further details on data analysis should refer to the existing review papers^{7,8} and the textbook.⁹

At a reactor source, most of neutron reflectometers^{10,11} use a monochromatic beam with constant λ and make a so-called θ - 2θ scan, in which the angles of a sample and a detector relative to the incident beam are simultaneously changed keeping the specular condition, to observe specular reflection. On the other hand, the reflectometers at a spallation neutron source with a proton accelerator^{8,12-14} or the ones installing a mechanical chopper at a reactor^{15,16} utilize white neutrons with a wide λ band as the incident beam. The obtained data is analyzed by using a Time-of-Flight (TOF) method. It should be noted that the pulsed-neutron reflectometer is able to measure specular reflection in a wide Q_z -range at one time according to the λ bandwidth without moving the sample. This means that the pulsed-neutron reflectometer is suitable for the studies on free interfaces if it adopts a horizontal-sample geometry, and also for a time-resolved measurement of reflectivity if the neutron source has high intensity in the incident beam. Moreover, a simultaneous measurement of off-specular as well as specular reflections is possible without any

scans by using simply a one-dimensional position-sensitive detector.

SOME EXPERIMENTAL EXAMPLES

Interfacial Structure of a Block Copolymer with a Lamellar Microdomain

A block and graft copolymers with incompatible components exhibit a highly-ordered self-assembled structure with a scale of *nm* in bulk or in a condensed solution. It has been clarified that the morphology and size of microdomains are dependent on the primary structure, *i.e.*, composition, molecular weight, and molecular architecture, of the block and graft copolymers.^{17–19} The static structure of phase-separated interfaces was precisely examined for AB diblock and BAB triblock copolymers composed of A = polystyrene (PS) and B = poly(2-vinylpyridine) (P2VP) at room temperature for the understanding of their self-assembled structure at the molecular level.^{20,21} All the block copolymers used here have total molecular weight of about 90×10^3 , and were confirmed to have an alternating lamellar structure in bulk, which is the simplest among the other morphologies of block and graft copolymers. The PS block chains in them were fully deuterated for the neutron experiment. The thin film specimens for reflectivity measurement were prepared by spin-coating the block copolymer solutions in a common good solvent on polished surface of silicon wafers, and then were annealed in a vacuum at high temperature well above T_g , $\sim 110^\circ\text{C}$, of the component polymers for a sufficiently long period of time to have thermodynamically equilibrium states in the films. Figure 2 shows a typical neutron specular reflectivity profile for the thin film of PS-P2VP diblock copolymer as a function of Q_z , along with the X-ray data for the same film specimen as the neutron. The neutron data possesses a few distinct

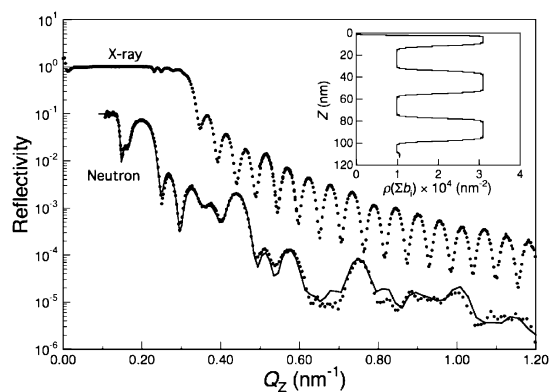


Figure 2. The neutron and X-ray specular reflectivity profiles for the thin film of a PS-P2VP diblock copolymer with a lamellar structure. The solid line on the neutron data is the best-fitted reflectivity calculated from the $\rho(\Sigma b_i)$ profile shown in the inset.

Bragg peaks originating from the structure ordered preferentially along the film depth direction, though the X-ray data shows only the Kiessig fringes reflecting total film thickness due to the small difference in electron density between the deuterated PS and P2VP. The best $\rho(\Sigma b_i)$ profile along the film depth direction, obtained from the model fitting analysis for the neutron data, is shown in the inset. From this $\rho(\Sigma b_i)$ profile, it was found that the deuterated PS and P2VP microdomains are alternatively stacked with a repeating distance of 43 nm in the 110 nm-thick film, and the lamellar structure is well oriented along the direction parallel to the film surface. The interfacial profile, $\phi_i(Z)$, between lamellae was well described by using an error function, and the interfacial thickness, L_{int} , defined as $(d\phi_i(Z)/dZ)$ at $\phi_i = 0.5$, was evaluated to be about 3.3 ± 0.3 nm for the PS-P2VP diblock copolymer. It was clarified that the L_{ints} thus evaluated for the BAB triblock copolymers of PS and P2VP are almost the same as that for the AB diblock irrespective of the difference in molecular architecture. Also, all the evaluated L_{ints} had much larger values than the prediction, 2.1 nm, by a mean-field theory taking the connectivity of the block chains into account,²² even though all the block copolymers were kept in the strong segregation state. This discrepancy between the experimental and theoretical values in interfacial thickness was quantitatively explained by considering the contribution of thermal fluctuations on polymer interface.^{23,24} Namely, the microphase-separated interfaces having inherent thickness for a pair of the components are considerably roughened by the thermal fluctuations during the annealing process at the temperature above T_g .

Moreover, Figure 3 shows a two-dimensional pattern of reflected neutron intensity obtained for the BAB triblock copolymer film of deuterated PS and P2VP showing a lamellar structure. Along the Q_z -direction at $Q_x = 0 \text{ nm}^{-1}$ a specular reflection ridge

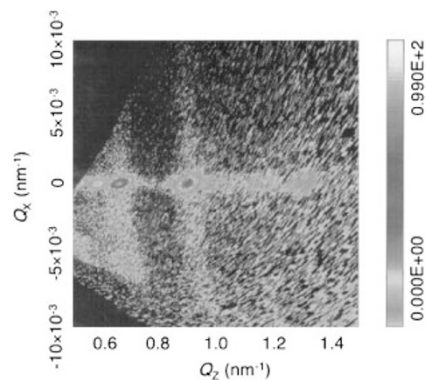


Figure 3. The two-dimensional pattern of reflected neutron intensity for the thin P2VP-PS-P2VP triblock copolymer film with a lamellar structure.

is observed, and the Bragg peak spots can be recognized at the position of $Q_Z = 0.65$ and 0.9 nm^{-1} . It should be noted that a weak off-specular reflection streaks are orthogonally crossing the specular ridge at the positions of the Bragg peaks. This implies that the phase-separated interfaces existing in the film are roughened by thermal fluctuations with some spatial correlation among them.

Localization of Component Chains in a Block Copolymer Blend with Wide Composition Distribution

For most of the studies on microphase-separated structure, block copolymers with narrow distribution in molecular weight and composition have been synthesized and used to examine the dependence of their self-assembled structure on the molecular parameters. On the other hand, the block copolymers used for practical application have generally wide molecular weight and composition distribution. It is interesting to investigate the effects of distribution in the molecular parameters on their physical properties. The previous morphological observation for polydisperse block copolymers in composition and molecular weight clarified that lamellar domain spacing increases linearly with increasing the polydispersity in molecular weight or composition.^{25–27} However, these results suggested only speculation on spatial distribution of the component block chains in microdomains. Thus, the segmental distribution of the component chains in block copolymer blends was directly examined by neutron reflectometry. The diblock copolymer of PS and P2VP with wide composition distribution was prepared by blending three pure monodisperse copolymers with the same molecular weights but different compositions, *i.e.*, the volume fraction of PS block chain in a molecule, f_{PS} , of 0.1, 0.5, and 0.9, at the blend ratio of 1:1:1 in weight to produce a lamellar structure for a reflectivity measurement.^{28,29} The three different deuterated ternary blends, whose compositions are exactly the same, were prepared. The blend-I was consisted of two unlabeled chains, of which f_{PS} are 0.1 and 0.5, and a labeled chain with f_{PS} of 0.9, while the blend-II included an unlabeled chain with f_{PS} of 0.1 and two remaining labeled chains. In the last blend-III all the three components were labeled. Figure 4 shows a neutron specular reflectivity profile for the thin spin-coated PS-P2VP film of the ternary blend-I, along with its $\rho(\Sigma b_i)$ profile obtained by the model fitting analysis. The $\rho(\Sigma b_i)$ profile exhibits broad peaks in PS lamellar microdomains with its peak values lower than that of pure deuterated PS. From this $\rho(\Sigma b_i)$ profile, it turned out that the longer block chain in the blend is localized at the center of a lamellar microdomain. On the other hand, the segmental distribution of the shorter block chain

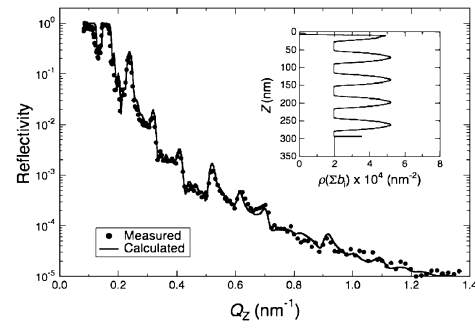


Figure 4. The neutron specular reflectivity profile for the PS-P2VP diblock copolymer blend (the ternary blend-I), along with the obtained $\rho(\Sigma b_i)$ profile shown in the inset.

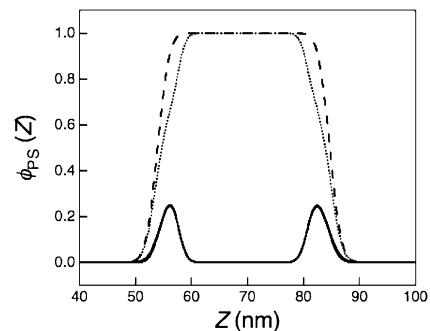


Figure 5. The volume fraction profile of the shorter block chains in a lamellar microdomain, with those experimentally obtained for the ternary blends-II and -III.

was estimated by a subtraction method based on incompressibility assumption, since the contrast is too low to obtain good statistics in reflectivity data if only the PS chain with $f_{\text{PS}} = 0.1$ is labeled in the blends. Hence, the volume fraction profile of the labeled PS segment obtained for the blend-II was subtracted from that for the blend-III as shown in Figure 5. It was found that the shorter block chains tend to be localized at the lamellar interface in the blend with wide composition distribution. The evaluated segmental distribution in the block copolymer blend supported the previous morphological observations well.^{25–27}

Interdiffusion Behavior of a Cyclic Polystyrene Compared with a Linear Homologue

A cyclic polymer has attracted much attention from the aspects of polymer physics due to its unique feature in molecular architecture with no chain ends. The existence of chain ends is essential for polymer dynamics such as diffusion and relaxation of a linear polymer chain in melt in the context of reptation theories.^{30,31} Then, a simple question arises how cyclic polymer can move without chain ends in melt. Here, the interdiffusion behavior of cyclic polymer was investigated through time evolution of interfacial broadening between the two polymer layers, and compared

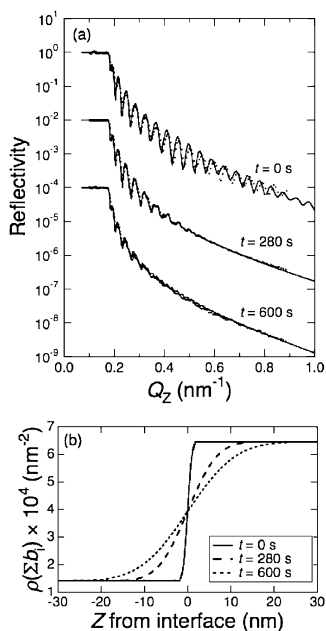


Figure 6. (a) The neutron specular reflectivity profiles for the (*l*-hPS/*c*-hPS/*c*-dPS) trilayer films with different annealing time. (b) The evaluated $\rho(\Sigma b_i)$ profiles for the interface between *c*-hPS and *c*-dPS layers.

with that of linear one by neutron reflectometry and dynamic secondary ion mass spectroscopy (DSIMS).³² The samples used were monodisperse cyclic and linear polystyrenes (*c*-hPS and *l*-hPS) having molecular weights of 116×10^3 , and their deuterated counterparts (*c*-dPS and *l*-dPS). It is noted that the molecular weight, M_e , between entanglements is 15×10^3 for linear polystyrene. The (*l*-hPS/*l*-dPS) bi- and (*l*-hPS/*c*-hPS/*c*-dPS) tri-layer films were prepared on silicon wafers by a floating method:^{33–35} a polymer film spin-coated on a glass slide was floated off on water surface, and then picked up by another polymer film separately prepared on a silicon wafer. These film specimens were annealed at 120 °C in a vacuum for different annealing time, and all the reflectivity measurements shown here were performed at room temperature. Figure 6(a) shows a series of specular neutron reflectivity profiles for the (*l*-hPS/*c*-hPS/*c*-dPS) trilayer films annealed in the different time from 0 to 600 s. It is apparent that the Kiessig fringe reflecting dPS layer thickness is damped off rapidly with increasing the annealing time, implying that the interface between the layers is broadened due to the interdiffusion of polymer chains. The best-evaluated $\rho(\Sigma b_i)$ profiles for the (*c*-hPS/*c*-dPS) interface shown in Figure 6(b) well support the above description on interfacial broadening. It was found that both the interfacial thicknesses, for cyclic and linear polymers increased with increasing the annealing time, t , and the interface for the cyclic one was broadened, that is, the cyclic polymer diffused, much faster than that for

the linear. The increment of interfacial thickness for the cyclic chain was proportional to $t^{0.19}$ at the shorter time, while it followed the Fickian diffusion (proportional to $t^{0.48}$) after reptation time, τ_d , around 3×10^3 s. Further, the diffusion coefficient, D , was evaluated from the interfacial profile obtained by DSIMS at the sufficiently longer time than τ_d . When the molecular weight is sufficiently higher than M_e , the value of D , $(1.1 \pm 0.1) \times 10^{-16}$ cm²/s, for the cyclic chain was about 2 times larger than that for the linear.

Temporal Interfacial Evolution for Miscible Poly(4-trimethylsilylstyrene)/polyisoprene Bilayer Films

Polymer interfaces play an important role in mechanical properties such as toughness and adhesion for multi-component systems. So far, many efforts have been paid to understand polymer interfaces and control their properties. A pair of poly(4-trimethylsilylstyrene) (PTMSS) and polyisoprene (PI) was recently discovered to be miscible and show phase-separation behavior with the lower critical solution temperature (LCST).^{36–38} Here, the compositional change in interface for the bilayer film of PTMSS and PI was observed in a real time by the *in-situ* neutron reflectivity measurement at 90 °C lower than the LCST in an inert gas environment.³⁹ Deuterium was introduced on a trimethylsilyl group in the PTMSS being substituted for hydrogen in neutron experiment. The bilayer film was prepared by the following floating method:^{33–35} the partially-deuterated PTMSS film was floated off onto water surface, and then picked up with the PI film spin-coated on a silicon wafer. Figure 7 shows temporal evolution of neutron specular reflectivity profile for every 5 min after the temperature jump to 90 °C. The Kiessig fringe with a relatively low frequency observed for the as-prepared bilayer film almost disappeared within about 10 min after the temperature jump, and then the different fringe with higher frequency was evolved. The solid lines are the best-fitted reflectivity profiles calculated from the $\rho(\Sigma b_i)$ profiles shown in Figure 8. The $\rho(\Sigma b_i)$ profile for the as-prepared bilayer film keeps a very sharp interface between the two layers. Just after the temperature jump the interface started to be broadened, and its position was moved toward the film surface due to the diffusion of mobile rubbery PI into glassy PTMSS. At the end, almost uniform $\rho(\Sigma b_i)$ was attained along the depth direction reflecting homogeneous composition, though the film surface was still kept enriched with the PTMSS with lower surface energy. This complicated interfacial behavior does not simply obey the Fickian diffusion process, but can be explained by an asymmetric diffusion⁴⁰ due to the difference in molecular mobility between glassy PTMSS and rubbery PI at 90 °C.

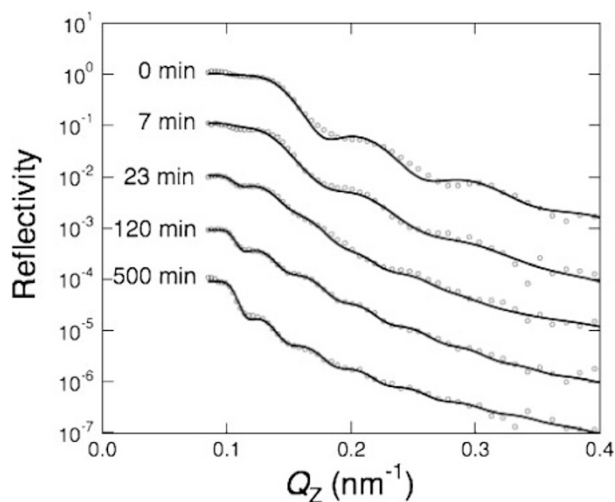


Figure 7. The time evolution of neutron specular reflectivity profile for the bilayer film of PTMSS/PI after the temperature jump to 90 °C.

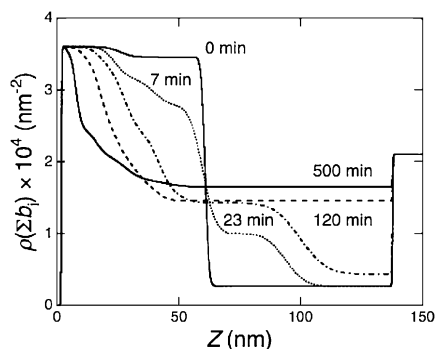


Figure 8. The change in $\rho(z)$ distribution along the Z-direction, obtained for the data shown in Figure 7 by a conventional model fitting method.

Phase Transition of a Thin Lipid Film with Salt on a Solid Substrate

The living cells and their organelle exist only as uni-lamellar vesicles (ULV) of phospholipids, so that the effective method to produce artificially the ULVs as a model biomembrane has been pursued. It was recently found that the addition of sugar or salt promotes the ULV formation only when they were mixed into the lipid films before hydration in the process of “natural swelling”.^{41–43} The stacking structure of lipid (dimyristoylphosphatidylcholine; DMPC) bilayers with NaI salt on a solid substrate was studied by using neutron reflectometry to understand the mechanism of the preferential ULV formation described above.^{44–46} Firstly, it was clarified by static measurements that NaI salt is intercalated between the lipid bilayers, and induces the phase transition to an “interdigitated” phase at the temperature above the chain-melting transition, around 60 °C, for a pure dry DMPC. Figure 9(a) shows the time dependence of neutron

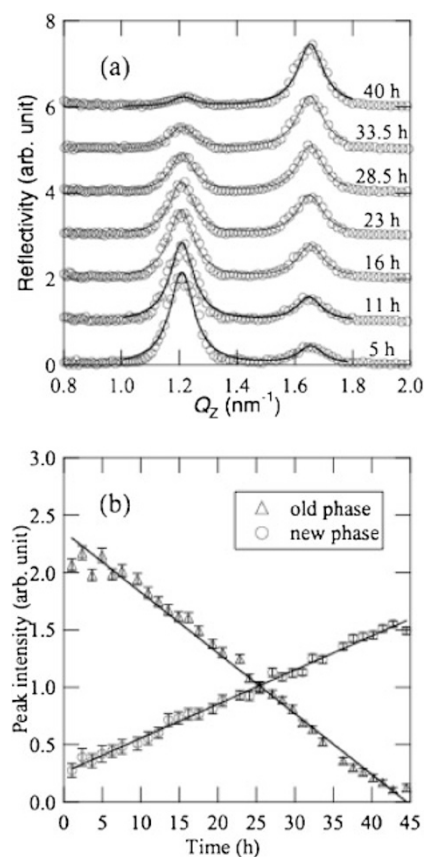


Figure 9. (a) The time dependence of neutron specular reflectivity profile for the thin film of a mixture of DMPC and NaI after the temperature jump to 120 °C. (b) The peak intensity evaluated for the two Bragg peaks as a function of annealing time.

reflectivity profile for a thin film of the DMPC/NaI mixture at the equi-molar ratio in a vacuum after a temperature jump to 120 °C.⁴⁵ The Bragg peak around $Q_Z = 1.2 \text{ nm}^{-1}$ at low temperature corresponds to the lipid bilayers with the salt intercalated between them, as clarified previously.⁴⁵ While the peak intensity of the Bragg peak around $Q_Z = 1.2 \text{ nm}^{-1}$ decreased, the one around $Q_Z = 1.65 \text{ nm}^{-1}$ newly developed with annealing time after the temperature jump. This new Bragg peak was assigned to the “interdigitated” phase, since the apparent bilayer thickness evaluated from the Bragg peak is too small to be explained for fully bent hydrocarbon chains of the lipid, and is almost equivalent to that for the “interdigitated” phase reported in the aqueous solutions.^{47,48} The correlation length along the depth direction, evaluated by the Bragg peak analysis,⁴⁹ was constant irrespective of the annealing time due to the spatial constraints in the thin film, so that the time dependence of the peak intensity should reflect the occupied area of each co-existing phase in the film plane. Figure 9(b) plots the peak intensity of the two Bragg peaks as a function of the annealing time. Both of the Bragg peaks showed the linear dependence on the time. This is ap-

parently different from the case in the aqueous solutions showing the exponential dependence.⁴⁸ The transition to the “interdigitated” phase in the thin lipid film exhibited the same phase growth behavior as the late stage spinodal decomposition in a two-dimensional space, of which phase growth in the occupied area is proportional to the annealing time.^{50,51}

FUTURE PROSPECTS

In this article, neutron reflectometry was reviewed by highlighting the actual experimental examples on the thin films of polymer and lipid. The neutron reflectometry itself is applicable to the other types of material interfaces such as liquid surface, liquid/liquid and solid/liquid interfaces. Many studies on the soft-material interfaces have been developed:^{52–61} monolayer systems of amphiphilic molecules on water surface, a polymer brush at solid/liquid interface, a hybrid polymer film with nanofillers, a polymer blend film, and so on, though they are not shown here. However, so far the adoption of neutron reflectometry has been limited due to a relatively small flux in the incident beam compared with a synchrotron X-ray source. Currently a high-intensity pulsed-neutron source is constructed in the project of Japan Proton Accelerator Research Complex (J-PARC), Tokai.⁶² The pulsed-neutron reflectometer with a horizontal sample-geometry⁶³ for free interfaces is proposed there, and expected to have at least a few hundreds times higher incident flux than the instruments^{12,13} at the KENS with the proton accelerator power of 5 kW. This big gain in incident flux would facilitate to make a time-resolved measurement of neutron reflectivity in seconds or minutes for time-dependent interfacial phenomena, and also the measurement of weak off-specular reflection for the in-plane structure of interfaces. Further, the installation of unique measurement options are discussed for the new reflectometer: a grazing-incidence diffraction or small-angle scattering option using a focused beam to explore the in-plane structures near surface region, and neutron spin-echo option with resonance spin flippers to observe interfacial dynamics directly.⁶⁴ New interfacial sciences are expected to develop much with a high-intensity pulsed-neutron beam.

The neutron reflectivity experiments shown here were performed under the Japan-UK Collaboration Program on Neutron Scattering, and the Inter-University Research Program on Pulsed-Neutron Scattering at Oversea Facilities. N. T. and N. Y. are indebted to the supports by a Grant-in-Aid for Creative Scientific Research (16GS0417) from the Ministry of Education, Culture, Sports, Science and Technology of Japan.

REFERENCES

1. R. A. L. Jones and R. W. Richards, in “Polymers at Surfaces and Interfaces,” Cambridge University Press, Cambridge, 1999.
2. A. Karim and S. Kumar, in “Polymer Surfaces, Interfaces and Thin Films,” World Scientific Publishing, Singapore, 2000.
3. A.-J. Dianoux and G. Lander, in “Neutron Data Booklet, Second Edition,” Old City Publishing, Philadelphia, 2003.
4. M. C. Wiener, S. Tristram-Nagle, D. A. Wilkinson, L. E. Campbell, and J. F. Nagle, *Biochim. Biophys. Acta*, **938**, 135 (1988).
5. L. G. Parratt, *Phys. Rev.*, **95**, 359 (1954).
6. M. Born and E. Wolf, in “Principles of Optics,” Oxford, Pergamon, 1970.
7. T. P. Russell, *Mater. Sci. Rep.*, **5**, 171 (1990).
8. J. Penfold and R. K. Thomas, *J. Phys.: Condens. Matter*, **2**, 1369 (1990).
9. J. Daillant and A. Gibaoud, in “X-Ray and Neutron Reflectivity: Principles and Applications,” Springer, New York, 1999.
10. T. Ebisawa, S. Tasaki, Y. Otake, H. Funahashi, K. Soyama, N. Torikai, and Y. Matsushita, *Physica B*, **213–214**, 901 (1995).
11. D. Yamazaki, K. Soyama, A. Moriai, I. Tamura, and K. Nakamura, *J. Jpn. Soc. Neutron Sci.*, **16**, 174 (2006) (in Japanese).
12. N. Torikai, M. Furusaka, H. Matsuoka, Y. Matsushita, M. Shibayama, A. Takahara, M. Takeda, S. Tasaki, and H. Yamaoka, *Appl. Phys. A*, **74**, S264 (2002).
13. M. Takeda and Y. Endoh, *Physica B*, **267–268**, 185 (1999).
14. J. Penfold, R. M. Richardson, A. Zerbakhsh, J. R. P. Webster, D. G. Bucknall, A. R. Rennie, R. A. L. Jones, T. Cosgrove, R. K. Thomas, J. S. Higgins, P. D. I. Fletcher, E. Dickinson, S. J. Roser, I. A. McLure, A. R. Hillman, R. W. Richards, E. J. Staples, A. N. Burgess, E. A. Simister, and J. W. White, *J. Chem. Soc., Faraday Trans.*, **93**, 3899 (1997).
15. R. Cubitt and G. Fragneto, *Appl. Phys. A*, **74**, S329 (2002).
16. M. James, A. Nelson, A. Brule, and J. C. Schulz, *J. Neutron Res.*, **14**, 91 (2006).
17. I. W. Hamley, in “The Physics of Block Copolymers,” Oxford University Press, Oxford, 1998.
18. Y. Matsushita, *J. Phys. Soc. Jpn.*, **65**, Suppl. A 119 (1996).
19. Y. Matsushita, *J. Polym. Sci., Part B: Polym. Phys.*, **38**, 1645 (2000).
20. N. Torikai, Y. Matsushita, S. Langridge, D. Bucknall, J. Penfold, and M. Takeda, *Physica B*, **283**, 12 (2000).
21. N. Torikai, M. Seki, Y. Matsushita, M. Takeda, K. Soyama, N. Metoki, S. Langridge, D. Bucknall, and J. Penfold, *J. Phys. Soc. Jpn.*, **70**, A 344 (2001).
22. K. R. Shull, *Macromolecules*, **25**, 2122 (1992).
23. K. R. Shull, A. M. Mayes, and T. P. Russell, *Macromolecules*, **26**, 3929 (1993).
24. M. Sferrazza, C. Xiao, R. A. L. Jones, D. G. Bucknall, J. Webster, and J. Penfold, *Phys. Rev. Lett.*, **78**, 3693 (1997).
25. Y. Matsushita, A. Noro, M. Iinuma, J. Suzuki, H. Ohtani,

- and A. Takano, *Macromolecules*, **36**, 8074 (2003).
26. A. Noro, M. Inuma, J. Suzuki, A. Takano, and Y. Matsushita, *Macromolecules*, **37**, 3804 (2004).
 27. A. Noro, D. Cho, A. Takano, and Y. Matsushita, *Macromolecules*, **38**, 4371 (2005).
 28. N. Torikai, A. Noro, M. Okuda, F. Odamaki, D. Kawaguchi, A. Takano, and Y. Matsushita, *Physica B*, **385–386**, 709 (2006).
 29. A. Noro, M. Okuda, F. Odamaki, D. Kawaguchi, N. Torikai, A. Takano, and Y. Matsushita, *Macromolecules*, **39**, 7654 (2006).
 30. P. G. de Gennes, *J. Chem. Phys.*, **55**, 572 (1971).
 31. M. Doi and S. F. Edwards, in “The Theory of Polymer Dynamics,” Oxford University Press, Oxford, 1986.
 32. D. Kawaguchi, K. Matsuoka, A. Takano, K. Tanaka, T. Nagamura, N. Torikai, R. M. Dalgliesh, S. Langrdige, and Y. Matsushita, *Macromolecules*, **39**, 5180 (2006).
 33. D. Kawaguchi, K. Tanaka, A. Takahara, T. Kajiyama, and S. Tasaki, *Macromolecules*, **34**, 6164 (2001).
 34. D. Kawaguchi, K. Tanaka, T. Kajiyama, A. Takahara, and S. Tasaki, *Macromolecules*, **36**, 1235 (2003).
 35. O. Urakawa, S. F. Swallen, M. D. Ediger, and E. D. von Meerwall, *Macromolecules*, **37**, 1558 (2004).
 36. M. Harada, T. Suzuki, M. Ohya, A. Takano, and Y. Matsushita, *Polym. J.*, **36**, 538 (2004).
 37. M. Harada, T. Suzuki, M. Ohya, D. Kawaguchi, A. Takano, and Y. Matsushita, *Macromolecules*, **38**, 1868 (2005).
 38. M. Harada, M. Ohya, T. Suzuki, D. Kawaguchi, A. Takano, and Y. Matsushita, *J. Polym. Sci., Part B: Polym. Phys.*, **43**, 1214 (2005).
 39. M. Harada, T. Suzuki, M. Ohya, D. Kawaguchi, A. Takano, Y. Matsushita, and N. Torikai, *J. Polym. Sci., Part B: Polym. Phys.*, **43**, 1486 (2005).
 40. H. C. Lin, I. F. Tsai, A. C.-M. Yang, M. S. Hsu, and Y. C. Ling, *Macromolecules*, **36**, 2464 (2003).
 41. J. P. Reeves and R. M. Dowben, *J. Cell Physiol.*, **73**, 49 (1969).
 42. M. Hishida, H. Seto, and K. Yoshikawa, *Chem. Phys. Lett.*, **411**, 267 (2005).
 43. K. Tsumoto and T. Yoshimura, in preparation.
 44. N. L. Yamada, N. Torikai, T. Nakai, M. Hishida, K. Sakurai, and H. Seto, *Physica B*, **385–386**, 719 (2006).
 45. N. L. Yamada and N. Torikai, *Thin Solid Film*, **515**, 5683 (2007).
 46. N. L. Yamada and N. Torikai, *Trans. Mater. Res. Soc., Jpn.*, **32**, 271 (2006).
 47. T. Adachi, H. Takahashi, K. Ohki, and I. Hatta, *Biophys. J.*, **68**, 1850 (1995).
 48. H. Seto, M. Hishida, H. Nobutou, N. L. Yamada, M. Nagao, and T. Takeda, *J. Phys. Soc. Jpn.*, **76**, 054602 (2007).
 49. F. Nallet, D. Roux, and S. T. Milner, *J. Phys. France*, **51**, 2333 (1990).
 50. P. S. Sahni, G. Dee, J. D. Gunton, M. Phani, J. L. Lebowitz, and M. Kalos, *Phys. Rev. B*, **24**, 410 (1981).
 51. L. Sung, A. Karim, J. F. Douglas, and C. C. Han, *Phys. Rev. Lett.*, **76**, 4368 (1996).
 52. E. Mouri, P. Kaewsaiha, K. Matsumoto, H. Matsuoka, and N. Torikai, *Langmuir*, **20**, 10604 (2004).
 53. E. Mouri, K. Matsumoto, H. Matsuoka, and N. Torikai, *Langmuir*, **21**, 1840 (2005).
 54. M. Ujihara, K. Mitamura, N. Torikai, and T. Imae, *Langmuir*, **22**, 3656 (2006).
 55. K. Mitamura, T. Imae, E. Mouri, N. Torikai, H. Matsuoka, and T. Nakamura, *J. Nanosci. Nanotechnol.*, **6**, 36 (2006).
 56. U-Ser Jeng, Tsang-Lang Lin, Kwanwoo Shin, Hsin-Yi Lee, Chia-Hung Hsu, Zau-Ann Chi, Ming Chih Shih, and N. Torikai, *J. Nanosci. Nanotechnol.*, **7**, 1406 (2007).
 57. M. Kobayashi, N. Hosaka, M. Kaido, A. Suzuki, N. Torikai, K. Ishihara, and A. Takahara, *Soft Matter*, **3**, 740 (2007).
 58. N. Hosaka, N. Torikai, H. Otsuka, and A. Takahara, *Langmuir*, **23**, 902 (2007).
 59. D. Kawaguchi, K. Tanaka, N. Torikai, A. Takahara, and T. Kajiyama, *Langmuir*, **23**, 7269 (2007).
 60. H. Yokoyama, T. Miyamae, S. Han, T. Ishizone, K. Tanaka, A. Takahara, and N. Torikai, *Macromolecules*, **38**, 5180 (2005).
 61. K. Niihara, U. Matsuwaki, N. Torikai, H. Atarashi, K. Tanaka, and H. Jinnai, *Macromolecules*, **40**, 6940 (2007).
 62. <http://j-parc.jp/>.
 63. N. Torikai, M. Furusaka, H. Matsuoka, Y. Matsushita, M. Shibayama, A. Takahara, M. Takeda, S. Tasaki, and H. Yamaoka, *Trans. Mater. Res. Soc., Jpn.*, **28**, 47 (2003).
 64. D. Yamazaki, K. Soyama, T. Ebisawa, M. Takeda, N. Torikai, S. Tasaki, and H. Matsuoka, *Physica B*, **356**, 229 (2005).



Naoya Torikai was born in 1968, and grown up in Nagoya. He received his B.S. in 1991 and Ph.D. degrees of engineering in 1997 from Nagoya University under the supervision of Professor Ichiro Noda. After that, he joined Neutron Science Laboratory (KENS), Institute of Materials Structure Science, High Energy Accelerator Research Organization (KEK) as a research assistant in 1997, and then promoted to an associate professor in 2003. He contributed much to the construction of the first dedicated neutron reflectometer with a horizontal-sample geometry at a pulsed neutron source of the KENS in Japan in cooperation with a group of polymer scientists, and developed the researches on soft-material interfaces by using reflectivity and small-angle scattering techniques with neutron and X-ray. Now, he is working for a new neutron reflectometer at the project of Japan Proton Accelerator Research Complex (J-PARC).



Norifumi L. Yamada was born in Fukuoka Prefecture, Japan in 1977. After graduation from Hiroshima University, he moved to Neutron Science Laboratory, High Energy Accelerator Research Organization (KEK) as a post-doc researcher in April 2005. He received his Ph.D. degree in December, 2005 from Hiroshima University under the supervision of Professor Takayoshi Takeda. His present research is the mechanism of self-assembled vesicle structures of synthesized phospholipid molecules in the water solution by using neutron scattering. He has much experience and skill in the experiments of small-angle neutron scattering (SANS), neutron spin-echo, and neutron reflectometry.



Atsushi Noro was born in Mie Prefecture, Japan in 1978. He graduated from Nagoya University in Japan with a B.S. in 2002. After that, he worked as a Ph.D. student under the direction of Prof. Yushu Matsushita at the same university, studying block copolymers and block-type supramacromolecules. During his Ph.D. work, he got a fellowship from Japan Society for the Promotion of Science (JSPS). He completed his Ph.D. work in 2006, and he had joined Prof. Timothy Lodge's group at the Department of Chemistry in University of Minnesota as a JSPS postdoc fellow since October in 2006. Currently, he is working as an Assistant Professor at the Department of Applied Chemistry in Nagoya University from October in 2007. His current interests are in nanostructures from block copolymers, block copolymers in ionic liquids, and supramolecular polymers.



Masashi Harada was born in Nagano, Japan in 1972. He received his B.E. degree in 1996 and M.E. degree in 1998 from the University of Tokyo under the direction of Prof. Toshio Nishi, and subsequently joined Toyota Central R&D Labs., Inc. His Ph.D. degree was conferred by Nagoya University under the supervision of Prof. Yushu Matsushita in 2005. His current research interests include the industrial application of neutron (and X-ray) reflectometry and small-angle scattering.



Daisuke Kawaguchi is currently an Assistant Professor of Applied Chemistry at Nagoya University. He was born in Shimane Prefecture, Japan in 1976. He received his B.Eng. degree in 1999 and Dr.Eng. degree in 2003 from Kyushu University under the direction of Prof. Tisato Kajiyama. Kawaguchi moved to Nagoya University as a research associate in 2003 (Professor Yushu Matsushita's group, Department of Applied Chemistry, Graduate School of Engineering). Present research interests are (1) aggregation structures at polymer surfaces and interfaces and (2) aggregation structures and dynamics of multi-component polymers. He is the author and the coauthor of 26 original papers.



Atsushi Takano was born in Nagaoka city, Niigata prefecture, Japan in 1963. He received his B.S. degree in 1985 from Nagaoka Technological University and Ph.D. degree in 1991 from Tokyo Institute of Technology. After joining Professor Yoshinobu Isono's group as a research associate in Nagaoka Technological University for eight years, he moved to Nagoya University in 1999 (Professor Yushu Matsushita's group) where he started his career as a polymer scientist in the field of polymer physics. He was promoted to associate professor in 2005 at the same university. Present research interests are (1) morphology control of block copolymers, and (2) solution- and bulk properties of cyclic polymers and their derivatives. He is The author and The coauthor of c.a. 70 original papers, and c.a. 10 patents.



Yushu Matsushita is currently a Professor of Applied Chemistry at Nagoya University and he is a Vice-President of Nagoya University since 2007. He was born in Aichi Prefecture, Japan in 1954. He earned a B.Eng. in 1977 in Synthetic Chemistry and a Dr.Eng. in Applied Chemistry, School of Engineering at Nagoya University under the direction of Prof. Mitsuru Nagasawa. Matsushita joined Nagoya University in 1982, he moved to the Institute for Solid State Physics, the University of Tokyo in 1994, he rejoined Nagoya University in 1999. He received Wiley Polymer Science Award from Society of Polymer Science Japan (SPSJ) in 1999, and also received the Award of the Society of Polymer Science, Japan in 2007, meanwhile he became a director of SPSJ in 2006. His measure is in precise molecular design and synthesis of well-defined block- and related multi-component polymers and morphology control of their hierarchical domain structures. He is the author and the coauthor of ca. 140 original papers, 35 reviews and books.